ISSN 2231-3478 (Print)
JUSPS-B Vol. 30(3), 30-39 (2018). Periodicity-Monthly
Section B
(Online) ISSN 2319-8052

JOURNAL OF ULTRA SCIENTIST OF PHYSICAL SCIENCES
An International Open Free Access Peer Reviewed Research Journal of Physical Sciences
website:- www.ultrascientist.org
Estd. 1989

Photocatalytic degradation of methylene blue dye under visible light and influence of H_2O_2 using hydrothermally synthesized ZnO nanorod array

HARISH. PUNAMCHAND. SURYAWANSHI[1] and DILIP. RAMSING. PATIL[1*]

[1]Nanomaterial Research Laboratory
R. C. Patel Arts, Comm. & Science College, Shirpur, (India)
Corresponding Author* **Email-** dr.drpatil@gmail..com
http://dx.doi.org/10.22147/jusps-B/300302

Acceptance Date 31st January, 2018, Online Publication Date 2nd March, 2018

Abstract

The photocatalytic degradation of organic waste using semiconductor photocatalyst under visible light has now received a great interest. The vertically aligned ZnO nanorod array (ZnO NRA) was grown on FTO substrate using hydrothermal method and its photocatalytic activity was also studied. The crystalline structure, morphology and optical properties of as synthesized ZnO NRA were studied by x-ray diffraction (XRD), field emission gun scanning electron microscope (FE-SEM), UV-Visible spectrophotometer and photoluminescence spectroscopy. The addition of small amount of hydrogen peroxide in dye solution inhibits the recombination of electrons and holes on the surface of ZnO nanorod; it also enhance the degradation rate. The average diameter and length of ZnO nanorods are 180 nm and 1.2 µm respectively. The photocatalytic dye degradation rate of ZnO NRA was increased with visible light in the presence of hydrogen peroxide. It was found the degradation efficiency of synthesized ZnO NRA was achieved up to 75% in 3 hour duration in the presence of hydrogen peroxide and visible light.

Key words : ZnO nanorod array; Hydrothermal; photocatalyst; oxygen vacancy; Visible photocatalyst; electron acceptor.

1. Introduction

In recent year photocatalytic degradation of organic compound using semiconductor photocatalyst has attracted a great interest in a research field. The organic compounds originated from textile industries are now a serious issue due to their recalcitrant and toxic nature. The conventional water treatment plants are

inefficient to preformed complete degradation and it produces harmful secondary pollution[11,13,19,24,27]. The TiO_2 is benchmark photocatalyst and widely used, But ZnO is also suitable alternative to TiO_2 due to its high photocatalytic degradation rate[28,33,34]. In photocatalytic process one- dimensional nanostructure grown on surface are in used and it does not required filtration and recovery process than powder form photocatalyst[17,26,30]. The various approaches have been done for the synthesis of ZnO nanorod structures on various substrate using chemical vapor deposition (CVD)[22], pulse laser deposition (PLD)[29], metal organic chemical vapor deposition (MOCVD)[33], physical vapor deposition (PVD)[32], molecular beam epitaxy (MBE)[31] as these methods are expensive, complex process and high temperature requirement and unsuitable for large scale production. The hydrothermal method is now cost effective and it requires low temperature.

The main drawback of ZnO is a wide band gap (3.37eV) and it absorbs only UV light and recombination of electron and hole on surface of catalyst limits the photocatalytic application in visible light. It can be overcome by doping of metal and nonmetal[6,23], semiconductor coupling[15] and surface medication via organic material[2]. In addition the defect formation of ZnO nanostructure such as oxygen and zinc vacancies or interstitial defects also plays important role in photocatalytic application in visible light region[5]. Up to now visible light active ZnO nanostructure photocatalyst has now been successfully synthesized using hydrothermal and microwave assisted hydrothermal process[1,4,7]. But the recombination of electron and hole on surface of ZnO nanorods inhibits the photocatalytic degradation rate under the influence of UV and Visible light. The influences of hydrogen peroxide in photocatalytic reaction not only inhibit recombination of electron and hole but extend photocatalytic degradation rate under visible light[21,25]. In earlier works the photocatalytic reactions are carried out using nanoparticles and influence of H_2O_2 was studied, but using ZnO nanostructures and influence of H_2O_2 on photocatalytic degradation rate was rarely studied.

In this work, ZnO nanorod array were synthesized on fluorine doped tin oxide (FTO) glass substrate initially coated with seed layer and ZnO nanorods were grown on hydrothermal method. The effects of temperature and growth time on the morphology of ZnO nanorod array were studied. The photocatalytic performance of the ZnO NRA and presence of H_2O_2 on degradation rate was also investigated under visible light.

2. Materials and Methods

2.1 Materials :

Zinc Nitrate ($Zn(NO_3)_2.6H_2O$) and Hexamine (HMT) were purchased from merck. For the growth of ZnO nanorod array fluorine doped tin oxide (FTO) glass plate was purchased from sigma Aldrich

2.2 Preparation of ZnO seed layer :

Initially, ZnO seed layer was deposited on FTO substrate with spin coating method. The colloidal solution was prepared using 5mM zinc acetate in absolute ethanol and stirred at room temperature. Before seed layer deposition FTO substrate initially cleaned by sonication in DI water, ethanol and isopropanol each solution in 15 min. The seed layer was deposited at spin speed 3000 rpm for 30 sec followed by heating substrate at 150^{o}C for 15 min and repeat this step for three times. The substrate was further annealed at 350^{o}C in box furnace for 20 min.

2.3 Synthesis of ZnO nanorod array :

The ZnO nanorod array was grown on seeded substrate with the help of hydrothermal method the stepwise process are shown in Fig. 1 The ZnO seed layer deposited on a FTO substrate immersed in a solution where

conducting side facing downwards. The aqueous growth solution was prepared by taking equimolar 30 mM of Zinc Nitrate hexahydrate (Merck, 99%) and hexamethylenetetramine (Merck, 99%) in 175 ml de-ionized water. The reactor temperature was set at 95°C for 3 hour. The substrate was removed and washed several times with DI water and dry at room temperature and dried at 250°C for 30 min to remove any trace organic impurities. The same step was repeated for 90°C with same growth time. The samples were named as Z1 and Z2 for 95°C and 90°C growth temperature.

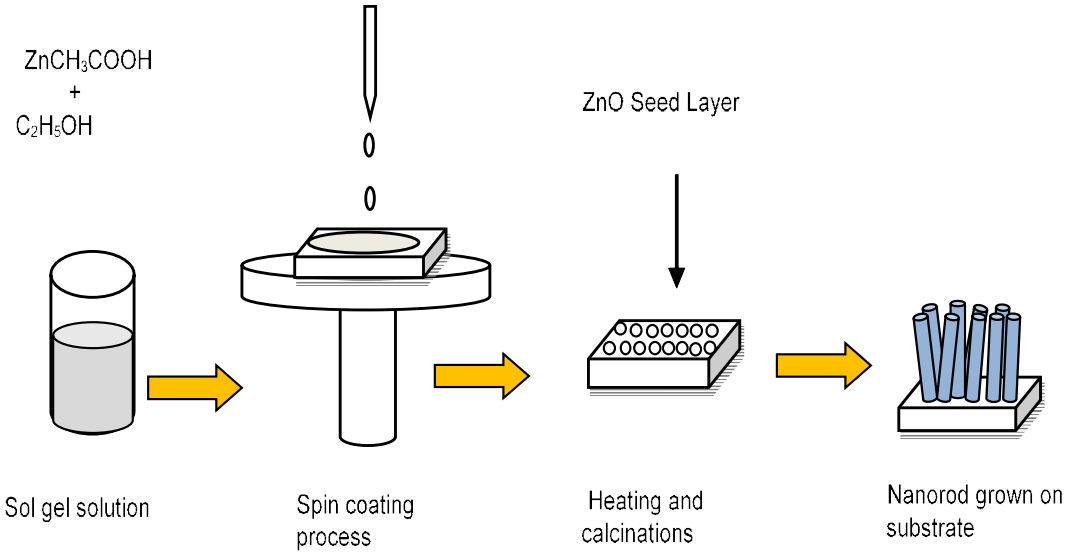

Fig.1 Stepwise process for synthesis of ZnO NRA

2.4 Characterization :

The crystal structure of ZnO nanorods array were evaluated by X-ray diffraction diffractometer (XRD) using Advanced D8 Bruker with CuKα radiation (λ=0.15405 nm) operated at a voltage 40 kV. The morphological study was done by FESEM (Hitachi S4800). The optical properties were studied using UV-Visible spectrophotometer (Shimadzu 2450) and Photoluminescence (PL) was measured with spectroflurometer (Fluoromax-4) with xenon lamp as excitation source. To evaluate the photocatalytic activities of ZnO nanorods array on FTO substrate (1 cm × 1cm) was immersed into 12 ml methylene blue aqueous solution in a glass beaker. This solution was irradiated by 100W incandescent Lamp for overall photocatalytic reaction. The sample was taken at every 30 min to measure the absorbance of dye solution.

3. Result and Discussion

3.1 Structural properties :

The XRD pattern of ZnO nanorod array using hydrothermal method shows in Fig 2(a). It was observed that the intense peak at an angle 33.67° indicate 002 plane for a sample synthesized at 95°C (Z1) than 90°C (Z2). It was observed that at 95°C the ZnO nanorods were grown anisotropically and remaining four peaks at an angle 30.9°, 33.7°, 36.8°, 47.6° which are assigned to the (100) (002) (101) and (102) plane. The XRD result shows that ZnO nanorod array having wurtzite structure with c-axis orientation.

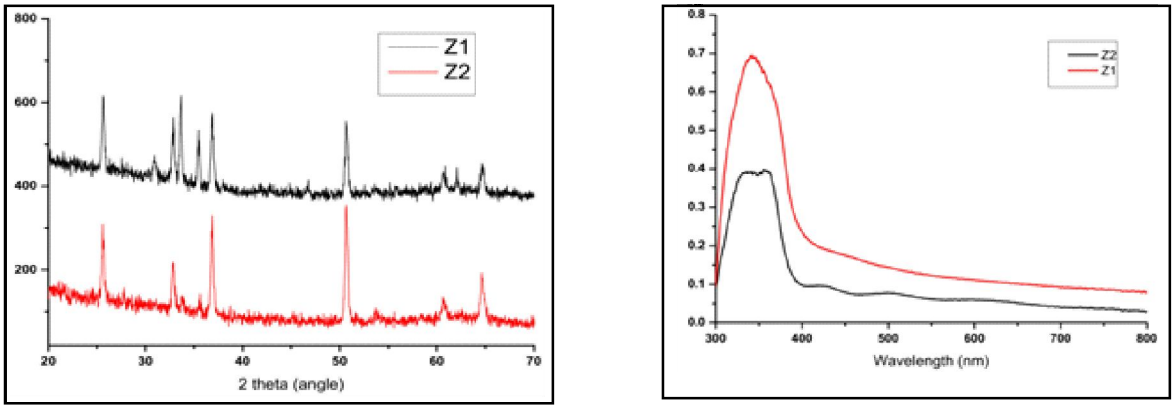

Fig. 2 (a) XRD pattern of ZnO nanorod array grown on FTO substrate and (b) UV-Visible absorbance of ZnO nanorod synthesized at 95^{o}C (Z1) and 90^{o}C (Z2) on FTO substrate.

3.2 Morphology :

The vertically aligned ZnO nanorod array morphological study were carried out using FE-SEM it shows in **Fig. 3** shows the SEM images of the prepared ZnO nanorod arrays grown on FTO substrate were shown at top view and cross sectional view. It was observed that the nanorods are vertically aligned with hexagonal structure and they were grown perpendicular direction on substrate. The ZnO nanorod array synthesized on FTO substrate with different growth temperatures are shown in figure below. The nanorod array grown at 90^{o}C are well aligned hexagonal structure the diameter and length of nanorods are 200 nm and 1µm respectively **Fig 3(a).** The ZnO nanorod array were grown at temperature 95^{o}C are well aligned, individually grown and perpendicular on FTO substrate with an average diameter and length was 150 nm and 1.2µm **Fig 3(b)** and **Fig 3(c)**. The cross section image (figure 3d) of ZnO NRA grown on FTO substrate shows the growth of nanorod is in perpendicular direction.

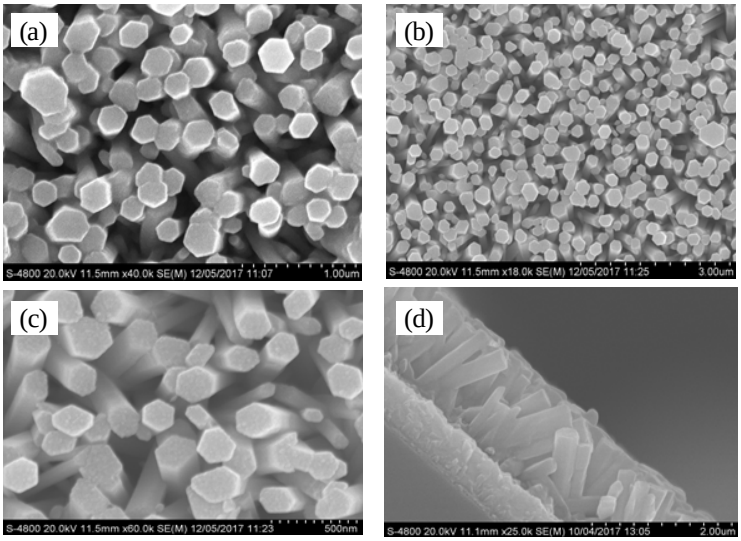

Fig. 3 The FESEM images on as synthesized ZnO nanorod array on FTO substrate grown at different growth temperature **(a)** 90^{o}C **(b)** 95^{o}C and (**c)** magnifying image of 95^{o}C sample. A typical cross section of ZnO nanorod array at 95^{o}C is shown in fig **(d)**.

3.3 Optical properties :

3.3.1 UV-Visible spectroscopy :

The UV-Visible spectra of ZnO nanorods array on FTO substrate with different growth temperatures are shown in Fig. 2 (b). It has been observed that ZnO NRA synthesized at 95^{o}C temperature have a slightly higher red shift as compared to nanorod array synthesized at 85^{o}C and 90^{o}C respectively. The UV absorption peak of ZnO nanorod array grown at 95^{o}C observed blue shift at wavelength from 300 nm to 325 nm. The optical band gap energy value of each nanorod array can be calculated by Tauc's plot method Fig 4 (b) The extrapolating straight line in the plot of $(Ahv)^2$ versus the photon energy (eV) for both ZnO nanorods array sample[14]. It indicates that the band gap energy decreases with increased in a growth temperature. The band gap of ZnO nanorod array was estimated at 95^{o}C is 3.17eV and for 90oC is 3.25eV. The gradual decrease in an optical band gap of ZnO nanorod indicates the band edge is red shifted and slight blue shift also observed in ZnO nanorod array due to oxygen vacancies present on ZnO nanorod surface[12].

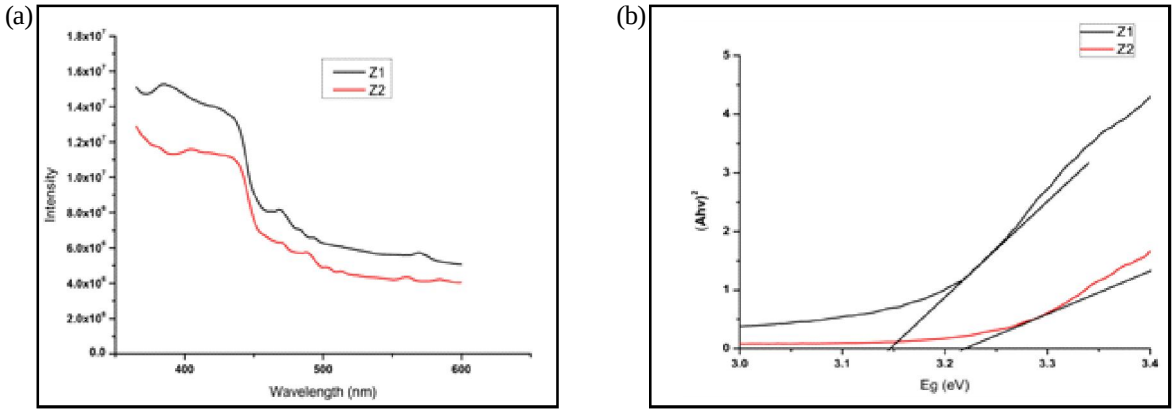

Fig. 4 (a) Photoluminescence spectra of ZnO NRA for Z1 and Z2 samples (b) Tauc plots of Z1 and Z2 samples.

3.3.2 Photoluminescence spectra :

The photoluminescence spectra of ZnO nanorod array grown at different growth temperatures are shown in Fig. 4(a). In both sample Z1 and Z2 the small emission peaks was observed at around ~386 nm in the spectrum due to the recombination of electron and hole pair in free exciton[8]. The small blue-green emission peak was observed at 468 nm in both samples Z1 and Z2 due to the surface defect or Zinc vacancy[18]. The intensity of blue-green emission peak of Z1 is greater than Z2. The weak green emission peak is observed at 570 nm that is possibly due to the oxygen vacancies[16] which is favorable to the photocatalytic reaction.

3.4 Photocatalytic activity of ZnO nanorod array :

In photocatalytic experiment, the ZnO nanorod array (NRA) grown on FTO substrate with dimension (1×1 cm) was used as photocatalyst. the methylene blue stock solution 8ml of was taken from 0.5mM stock solution with addition of 8ml distilled water in a 20 ml glass beaker and photocatalyst film was immersed by facing in coating side of film towards light source. The solution was kept in a dark condition for 30 min duration for achieving adsorption desorption equilibrium. A 100W incandescent lamp was used in overall photocatalytic

reaction. The water jar kept in between lamp and solution to avoid evaporation of dye solution due to heating effect of infrared and UV light. The 4ml of sample was taken at every 30 min interval for absorbance measurement and after measuring absorbance the solution was again returned to the beaker for next observation.

It was observed that the absorbance peak intensity of methylene blue solution was decreased with continuous irradiation of visible light as shown in Fig. 5. The photocatalytic degradation efficiency was calculated by the following equation

$$\eta = C0 - Ct/C0$$

Where, C_0 and C_t are the original concentrations of MB and change in concentration after visible light irradiation with time.

3.5 Effect of pH and H_2O_2 :

The photocatalytic reaction of ZnO NRA was evaluated with three different conditions. In first one the pH of methylene blue solution was kept at pH=8, second case 20mM of H2O2 was added in solution and pH changes to 6 and the last case photolysis effect was studied without using photocatalyst. The dye solution can be degraded under the influence of UV light and hydrogen peroxide due to the photolysis reaction[10]. The Table 1 shows different types of conditions have been taken in photocatalytic reaction for the ZnO nanorod array synthesized at 95°C and 90°C.

Table 1. A sample names of ZnO NRA at different growth temperature and influence of H_2O_2

Samples	Growth temperature	pH	H_2O_2 concentration
Z18	95°C	8	–
Z28	90°C	8	–
Z1H	95°C	6	20mM
Z2H	90°C	6	20mM

In photocatalytic experiment, it was observed that the ZnO NRA sample Z1H and Z2H shown highest degradation efficiency of 79% and 68% under visible light within 3 hour in the presence of H_2O_2 solution (Fig. d, e). The sample Z1H was shown higher photocatalytic activity in presence of H_2O_2 under the visible light. This photocatalytic activity of hydrothermally synthesized ZnO NRA was found to be higher with less growth time than reported work, utilized visible[4] and UV light source[9]. In another case, the dye solution of pH 8 the degradation efficiency of samples Z18 and Z28 are 48% and 47% respectively which is lower than the presence of H_2O_2 solution. At higher pH range the photocatalytic reaction rate is increase due to the formation of •OH radical from hydroxide.

The dye solution can be degraded in presence of visible light without photocatalyst named as photolysis degradation. To measure the photolysis rate of dye solution separate reaction was carried out without ZnO NRA samples with irradiation of visible light for 3 h irradiation exposure time. It was found that the methylene blue degradation rate was lower in the range of 15-20% smaller than pH 8 and H_2O_2 condition. This degradation was performed due to presence of H_2O_2 causes photolytic cleavage in presence of light and it decompose the dye molecules. It was also found that methylene blue was completely degraded after 1-2 day in presence of H_2O_2 at room temperature and precipitation of methylene blue compound was observed at the bottom of a beaker. But, in presence of ZnO NRA the degradation rate was enhanced in visible light without any precipitation. In a semiconductor photocatalyst when photon energy is equal to band gap energy, the electron

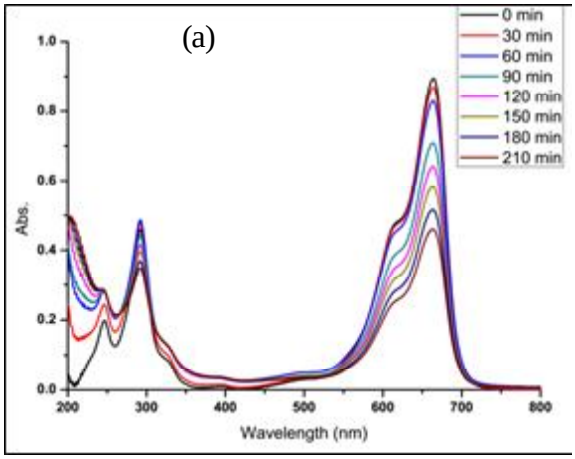
(a)
0 min
30 min
60 min
90 min
120 min
150 min
180 min
210 min
Abs.
Wavelength (nm)

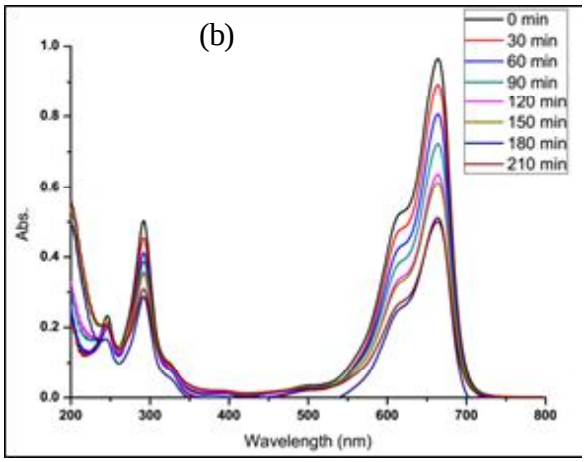
(b)
0 min
30 min
60 min
90 min
120 min
150 min
180 min
210 min
Abs.
Wavelength (nm)

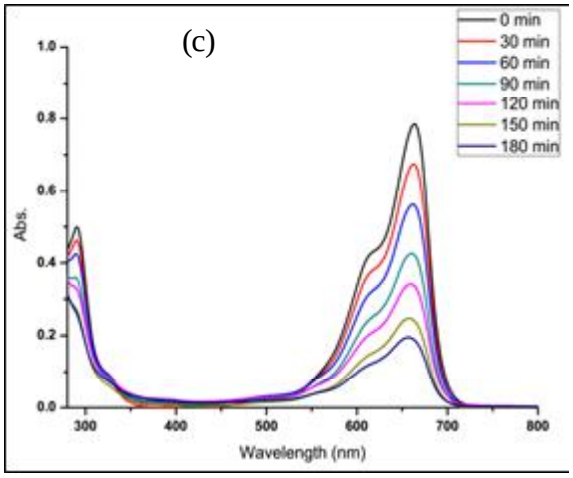
(c)
0 min
30 min
60 min
90 min
120 min
150 min
180 min
Abs.
Wavelength (nm)

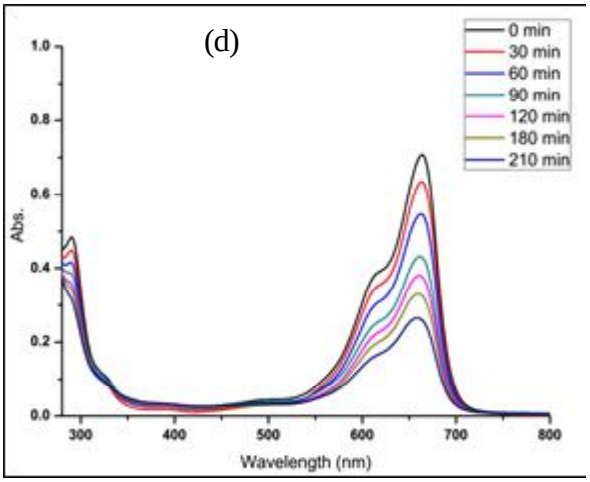
(d)
0 min
30 min
60 min
90 min
120 min
180 min
210 min
Abs.
Wavelength (nm)

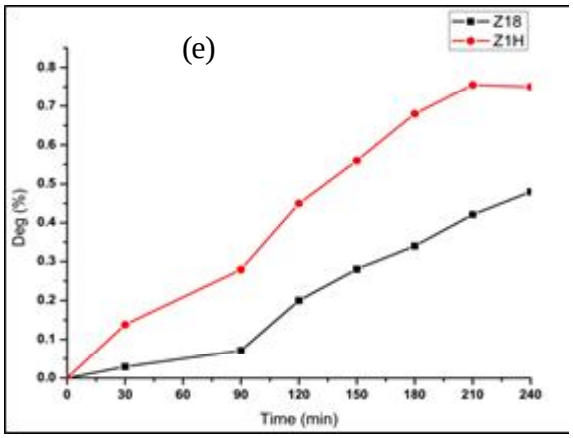
(e)
Z1B
Z1H
Deg (%)
Time (min)

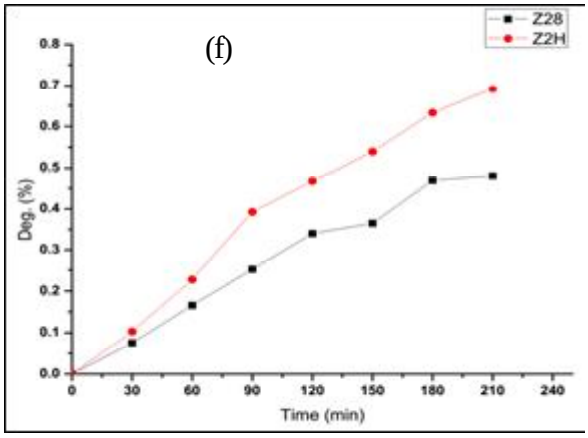
(f)
Z2B
Z2H
Deg. (%)
Time (min)

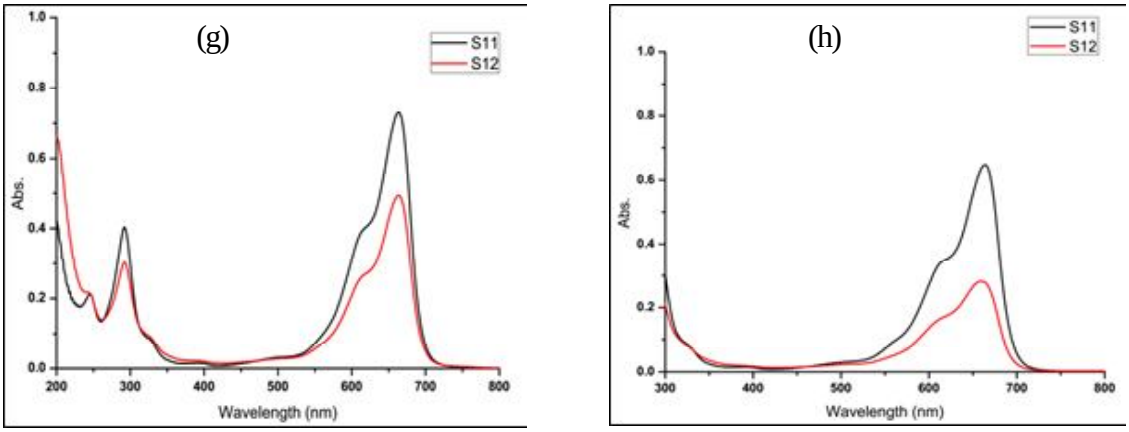

Fig. 5 The absorbance of photocatalytic degradation of methylene blue solution at pH=8 using ZnO NRA samples Z18 (a) and Z28 (b). The absorbance of ZnO NRA samples under influence of H_2O_2 in dye solution are Z1H (c) and Z2H (d). The plot of percentage degradation with time for both conditions of Z1 sample is shown in (d) and for Z2 sample (e). The Photolysis condition without ZnO NRA at pH 8 (g) and presence of H_2O_2 (h).

in valance band excited to conduction band with leaving hole behind. These photo-generated electron and hole recombine, some are traps in defect state or react with adsorbed water and dye molecule adsorbed on surface of photocatalyst. The electron and hole recombination inhibits the photocatalytic reaction; surface defects such as oxygen vacancies prevent recombination at certain limit. To prevent this issue the hydrogen peroxide was added into the dye solution in presence of ZnO NRA it acts as electron scavenger. The H_2O_2 capture the photo-induced electron on the surface of ZnO NRA and suppress the rate of electrons and holes reaction and produces •OH radical[20] shown in reaction (1). The hydrogen peroxide can able to generate •OH radical either conduction band electron or via superoxide radical ions as shown in reaction (2-3). It can be shown by following reactions.

$$ZnO\ (e_{CB}^{-}) + H_2O_2 \longrightarrow ZnO + {\bullet}OH + OH^{-} \quad (1)$$

$$H_2O_2 + e^{-} \longrightarrow {}^{\bullet}OH + OH^{-} \quad (2)$$

$$H_2O_2 + O_2^{-\bullet} \longrightarrow {}^{\bullet}OH + OH^{-} + O_2 \quad (3)$$

$$H_2O_2 \longrightarrow 2{}^{\bullet}OH \quad (4)$$

$$H_2O_2 \longrightarrow O_2^{2-} + 2H^{+} \quad (5)$$

In the absence of photocatalyst (ZnO NRA) the dye degradation occur in the presence of H_2O_2 by visible light irradiation. The reason behind is when H_2O_2 irradiated with visible light photolytic cleavage of H_2O_2 occur and it produces •OH radical shown in reaction (4-5) but the degradation rate is to slow.

4. Conclusion

The vertically aligned and hexagonal wurtzite structure ZnO nanorod array was grown on FTO substrate with the help of hydrothermal method. The PL spectra of ZnO also show blue and green emission, indicates

Zinc and oxygen vacancies or interstitial defects. Those defects are favorable in photocatalytic application. The ZnO NRA shows enhanced photocatalytic activity under the influence of visible light. The effect of pH and presence of H_2O_2 in dye solution increases the degradation rate under visible light. The ZnO NRA synthesized at 95^oC shows higher in photocatalytic degradation rate up 79% within 3 hour under visible light in presence of hydrogen peroxide. The dye solution was self degraded in presence of H_2O_2 and visible light but the degradation rate is lower compared to the presence of ZnO nanorod array. This method saves growth time and offers cost effective solution for the degradation of dyes in textile water using visible light.

Acknowledgment

The authors are thankful to Management of R. C. Patel Educational Trusts, Shirpur for providing research facilities.

References

1. Al-Sabahi J., Bora T., Al-Abri M., Dutta J., Controlled defects of zinc oxide nanorods for efficient visible light photocatalytic degradation of phenol. Materials *9*, 238 (2016).
2. An S., Joshi B.N., Lee M.W., Kim N.Y., Yoon S.S., Electrospun graphene-ZnO nanofiber mats for photocatalysis applications. Applied Surface Science *294*, 24-28 (2014).
3. Ashraf S., Jones A.C., Bacsa J., Steiner A., Chalker P.R., Beahan P., Hindley S., Odedra R., Williams P.A., Heys P.N., MOCVD of vertically aligned ZnO nanowires using bidentate ether adducts of dimethylzinc. Chemical Vapor Deposition *17*, 45-53 (2011).
4. Baruah S., Mahmood M.A., Myint M.T.Z., Bora T., Dutta J., Enhanced visible light photocatalysis through fast crystallization of zinc oxide nanorods. Beilstein journal of nanotechnology *1*, 14 (2010).
5. Baruah S., Sinha S.S., Ghosh B., Pal S.K., Raychaudhuri A., Dutta J., Photoreactivity of ZnO nanoparticles in visible light: Effect of surface states on electron transfer reaction. Journal of Applied Physics *105*, 074308 (2009).
6. Bhuyan T., Khanuja M., Sharma R., Patel S., Reddy M., Anand S., Varma A., A comparative study of pure and copper (Cu)-doped ZnO nanorods for antibacterial and photocatalytic applications with their mechanism of action. Journal of Nanoparticle Research *17*, 288 (2015).
7. Bora T., Sathe P., Laxman K., Dobretsov S., Dutta J., Defect engineered visible light active ZnO nanorods for photocatalytic treatment of water. Catalysis Today 284, 11-18 (2017).
8. Djurišiæ A.B., Leung Y.H., Optical properties of ZnO nanostructures. small *2*, 944-961 (2006).
9. Fragalà M.E., Di Mauro A., Cristaldi D.A., Cantarella M., Impellizzeri G., Privitera V., ZnO nanorods grown on ultrathin ZnO seed layers: Application in water treatment. Journal of Photochemistry and Photobiology A: Chemistry *332*, 497-504 (2017).
10. Galindo C., Jacques P., Kalt A., Photodegradation of the aminoazobenzene acid orange 52 by three advanced oxidation processes: UV/H 2 O 2, UV/TiO 2 and VIS/TiO 2: comparative mechanistic and kinetic investigations. Journal of Photochemistry and Photobiology A: Chemistry *130*, 35-47 (2000).
11. Ghoreishi S., Haghighi R., Chemical catalytic reaction and biological oxidation for treatment of non-biodegradable textile effluent. Chemical Engineering Journal *95*, 163-169 (2003).
12. Gupta J., Barick K., Bahadur D., Defect mediated photocatalytic activity in shape-controlled ZnO nanostructures. Journal of Alloys and Compounds *509*, 6725-6730 (2011).
13. Hameed B., Din A.M., Ahmad A., Adsorption of methylene blue onto bamboo-based activated carbon: kinetics and equilibrium studies. Journal of hazardous materials *141*, 819-825 (2007).
14. Hassanien A., Akl A.A., Influence of composition on optical and dispersion parameters of thermally evaporated non-crystalline Cd 50 S 50" x Se x thin films. Journal of Alloys and Compounds *648*, 280-290

(2015).
15. Hernández S., Cauda V., Hidalgo D., Rivera V. F., Manfredi D., Chiodoni A., Pirri F.C., Fast and low-cost synthesis of 1D ZnO–TiO 2 core–shell nanoarrays: characterization and enhanced photo-electrochemical performance for water splitting. Journal of Alloys and Compounds *615*, S530-S537 (2014).
16. Jin B., Bae S., Lee S., Im S., Effects of native defects on optical and electrical properties of ZnO prepared by pulsed laser deposition. Materials Science and Engineering: B *71*, 301-305 (2000).
17. Kamat P.V., Huehn R., Nicolaescu R., A "sense and shoot" approach for photocatalytic degradation of organic contaminants in water. The Journal of Physical Chemistry B *106*, 788-794 (2002).
18. Lin-Li Z., Chang-Xin G., Jian-Gang C., Jun-Tao H., The synthesis of one-dimensional controllable ZnO microrods. Chinese Physics *14*, 586 (2005).
19. McMullan G., Meehan C., Conneely A., Kirby N., Robinson T., Nigam P., Banat I., Marchant R., Smyth W., Microbial decolourisation and degradation of textile dyes. Applied microbiology and biotechnology *56*, 81-87 (2001).
20. Neppolian B., Choi H., Sakthivel S., Arabindoo B., Murugesan V., Solar light induced and TiO 2 assisted degradation of textile dye reactive blue 4. Chemosphere *46*, 1173-1181 (2002).
21. Pichat P., Guillard C., Amalric L., Renard A.-C., Plaidy O., Assessment of the importance of the role of H_2O_2 and O2o– in the photocatalytic degradation of 1, 2-dimethoxybenzene. Solar energy materials and solar cells *38*, 391-399 (1995).
22. Protasova L., Rebrov E., Choy K., Pung S., Engels V., Cabaj M., Wheatley A., Schouten J., ZnO based nanowires grown by chemical vapour deposition for selective hydrogenation of acetylene alcohols. Catalysis Science & Technology *1*, 768-777 (2011).
23. Rajbongshi B.M., Ramchiary A., Samdarshi S., Influence of N-doping on photocatalytic activity of ZnO nanoparticles under visible light irradiation. Materials Letters *134*, 111-114 (2014).
24. Robinson N.J., Whitehall S.K., Cavet J.S., Microbial metallothioneins. Advances in microbial physiology *44*, 183-213 (2001).
25. Samsudin E.M., Goh S.N., Wu T.Y., Ling T.T., Evaluation on the Photocatalytic Degradation Activity of Reactive Blue 4 using Pure Anatase Nano-TiO2. Sains Malaysiana *44*, 1011-1019 (2015).
26. Singh D.P., Synthesis and growth of ZnO nanowires. Science of Advanced Materials *2*, 245-272 (2010).
27. Slokar Y.M., Le Marechal A.M., Methods of decoloration of textile wastewaters. Dyes and pigments *37*, 335-356 (1998).
28. Tanaka K., Padermpole K., Hisanaga T., Photocatalytic degradation of commercial azo dyes. Water research *34*, 327-333 (2000).
29. Tien L., Pearton S., Norton D., Ren F., Synthesis and microstructure of vertically aligned ZnO nanowires grown by high-pressure-assisted pulsed-laser deposition. Journal of Materials Science *43*, 6925-6932 (2008).
30. Udom I., Ram M.K., Stefanakos E.K., Hepp A.F., Goswami D.Y., One dimensional-ZnO nanostructures: synthesis, properties and environmental applications. Materials science in semiconductor processing *16*, 2070-2083 (2013).
31. Wang J., Yang C., Chen P., Su C., Chen W., Chiu K., Chou W., Catalyst-free highly vertically aligned ZnO nanoneedle arrays grown by plasma-assisted molecular beam epitaxy. Applied Physics A *97*, 553 (2009).
32. Wang L., Zhang X., Zhao S., Zhou G., Zhou Y., Qi J., Synthesis of well-aligned ZnO nanowires by simple physical vapor deposition on c-oriented ZnO thin films without catalysts or additives. Applied Physics Letters *86*, 024108 (2005).
33. Zhai B.-g., Huang Y.M., A review on recent progress in ZnO based photocatalysts. Optoelectron Mater *1*, 22-36 (2016).
34. Zhang Y., Ram M.K., Stefanakos E.K., Goswami D.Y., Synthesis, characterization, and applications of ZnO nanowires. Journal of Nanomaterials 2012:20 (2012).